Granzyme K Expressed by Classically Activated Macrophages Contributes to Inflammation and Impaired Remodeling

Christopher T. Turner[1,2], Matthew R. Zeglinski[1,2], Katlyn C. Richardson[1,2], Hongyan Zhao[1,2], Yue Shen[1,2], Anthony Papp[3,5], Phillip I. Bird[4] and David J. Granville[1,2,5]

Granzyme K (GzmK), traditionally described as a pro-apoptotic, granule-secreted serine protease, has been proposed to promote inflammation. Found at low levels in the plasma of healthy individuals, GzmK is markedly elevated in response to sepsis and infection. In this study we investigated the role of GzmK in inflammation and remodeling in response to thermal injury. In human burn tissue, GzmK was elevated compared with normal skin, with expression predominantly found in macrophages. GzmK was expressed and secreted by cultured human classically activated macrophages. To assess the role of GzmK in response to skin wounding, wild-type or GzmK$^{-/-}$ mice were subjected to grade 2 thermal injury. GzmK$^{-/-}$ mice exhibited improved wound closure, matrix organization, and tensile strength compared with wild-type mice. Reduced proinflammatory IL-6, ICAM-1, VCAM-1, and MCP-1 expressions were observed at 3 days after injury. Additionally, GzmK induced IL-6 expression in keratinocytes and skin fibroblasts that was dependent on PAR-1 activation. Re-epithelialization showed the greatest degree of improvement of all healing parameters, suggesting that keratinocytes are sensitive to GzmK-mediated proteolysis. In support, keratinocytes, but not skin fibroblasts, exposed to GzmK showed impaired wound healing in vitro. In summary, GzmK influences wound healing by augmenting inflammation and impeding epithelialization.

Journal of Investigative Dermatology (2019) **139,** 930–939; doi:10.1016/j.jid.2018.09.031

INTRODUCTION

Granule-secreted enzymes (called *granzymes*) are a family of serine proteases long proposed to contribute to perforin-dependent cytotoxic T lymphocyte and natural killer (NK) granule exocytosis-mediated cell death (Lobe et al., 1986; Masson and Tschopp, 1987; Tschopp et al., 1986). There are five granzymes in humans: granzyme A (tryptase), granzyme B (aspartase), granzyme H (chymase), granzyme K (GzmK, tryptase), and granzyme M (metase). Each granzyme is uniquely expressed by different cell types, and each has separate substrate specificities and function(s) (reviewed by Turner et al., 2017a; Voskoboinik et al., 2015).

Emerging evidence challenges the notion that GzmK is cytotoxic and suggests that it may actually act to promote proinflammatory cytokine release (Joeckel et al., 2011, 2017). Although GzmK occurs at low levels in the plasma of healthy individuals, it is acutely elevated in response to viral infection (Bade et al., 2005), allergic asthma, pneumonia (Bratke et al., 2008), sepsis (Rucevic et al., 2007), and endotoxemia (Wensink et al., 2016). Mice infected with either lymphocytic choriomeningitis (Joeckel et al., 2017) or Chikungunya virus (Wilson et al., 2017) also show increased GzmK expression in plasma-derived cytotoxic T lymphocytes and plasma, respectively. GzmK$^{-/-}$ mice exhibit reduced foot swelling in response to Chikungunya virus infection (Wilson et al., 2017). Exposure of cultured lung fibroblasts and endothelial cells to GzmK stimulates proinflammatory cytokine release that is dependent on PAR-1 activation (Cooper et al., 2011; Sharma et al., 2016). GzmK also induces IL-1β production in macrophages (Joeckel et al., 2011).

Inflammation plays a key role in the development of excessive scarring and painful skin contractures caused by thermal/burn injury. Burn healing requires an intricate coordination of events involving interaction between multiple cell types and the extracellular microenvironment. Curbing excessive inflammation is a major strategy to reduce secondary burn wound expansion, scarring, and fibrosis. By augmenting inflammation, GzmK may provide an important contribution to the healing of burn wounds. In this study, GzmK was elevated in burn wounds, impaired healing through a process involving enhanced inflammation, and impaired remodeling.

RESULTS

GzmK was elevated in human burns and secreted by classically activated macrophages

GzmK expression was evaluated in human acute burn tissues excised from day 2 to day 30 after injury (see Supplementary

[1]*International Collaboration On Repair Discoveries (ICORD) Centre, Vancouver Coastal Health Research Institute, University of British Columbia, Vancouver, British Columbia, Canada;* [2]*Department of Pathology and Laboratory Medicine, University of British Columbia, Vancouver, British Columbia, Canada;* [3]*Department of Surgery, University of British Columbia, Vancouver, British Columbia, Canada;* [4]*Department of Biochemistry and Molecular Biology, Biomedicine Discovery Institute, Monash University, Melbourne, Australia; and* [5]*British Columbia Professional Firefighters' Burn and Wound Healing Group, Vancouver, British Columbia, Canada*

Correspondence: David J. Granville, International Collaboration On Repair Discoveries (ICORD) Centre, Blusson Spinal Cord Centre, Room 4470, 818 West 10th Avenue, Vancouver, British Columbia, V5Z 1M9, Canada. E-mail: david.granville@hli.ubc.ca

Abbreviations: GzmK, granzyme K; rhGzmK, recombinant human granzyme K; NK, natural killer; WT, wild type

Received 8 June 2018; revised 18 September 2018; accepted 21 September 2018; accepted manuscript published online 3 November 2018; corrected proof published online 11 January 2019

Table S1 online). In healthy undamaged skin, GzmK$^+$ cells were minimally dispersed throughout the dermis (Figure 1a). In contrast, partial thickness burn-injured skin exhibited increased numbers of GzmK$^+$ cells, with the vast majority localized to the inflammatory cell infiltrate but also in close proximity to the dermal-epidermal junction. The amount and localization of GzmK$^+$ cells was similar between all nine burn samples, despite differences in time after injury, wound location, and wound severity.

GzmK strongly co-localized with CD68$^+$ cells (marker of circulating monocyte and tissue macrophages) within burn tissue (Figure 1b). A separate GzmK$^+$ cell population was also observed in the burn wound tissue (Figure 1b), albeit with reduced GzmK staining intensity. This cell population was not identified.

Within differing stages of wound repair, multiple polarized subtypes of macrophages have been identified, each performing unique roles in inflammation, including proinflammation (M1) and prohealing (M2) (Murray, 2017). The macrophage subtype(s) responsible for GzmK expression was therefore investigated. M1 macrophages exhibited GzmK immune-positivity, with negligible staining observed in M2a macrophages (Figure 1c). Only classically activated M1 macrophages expressed GzmK mRNA (Figure 1d), as supported by immunofluorescence microscopy. GzmK secretion was also markedly elevated in M1 macrophages, but negligible levels were released by M2a macrophages (Fig. 1e).

Improved wound healing in GzmK$^{-/-}$ Mice

GzmK$^{-/-}$ and wild-type (WT) mice were subjected to thermal injury on the dorsum of 8-week-old female mice. Wounds were partial thickness (grade 2b), as shown by tissue damage penetrating into the dermis but not the muscle layer (Figure 2d), as reported previously (Shen et al., 2012). Negligible GzmK immune reactivity was evident in healthy control skin, but GzmK$^+$ cells were detected in WT mouse burns at days 3 and 6, localizing to the inflammatory cell infiltrate at the wound margin (Figure 2e). GzmK immune reactivity was absent in GzmK$^{-/-}$ mice burns. Macroscopically, there was a significant reduction in both wound area ($P < 0.005$) (Figure 2a and b) and wound gape ($P < 0.05$) (see Supplementary Figure S1 online) from day 5 until day 10 after injury in GzmK$^{-/-}$ compared with WT mice. Histological assessment supported the macroscopic data, showing a significant reduction in wound gape at day 6 ($P < 0.005$) (Figure 2c and d).

Re-epithelialization after injury was significantly improved in GzmK$^{-/-}$ mice at both days 3 and 6 compared with WT mice ($P < 0.005$) (Figure 3a). Supporting enhanced re-epithelialization, scabs were observed to drop off GzmK$^{-/-}$ mice wounds approximately two days (25%) earlier than WT controls (Figure 3b).

Masson's trichrome staining of GzmK$^{-/-}$ burn wounds at day 14 after injury showed improved collagen maturation within the wounded dermal area compared with that in WT mice ($P < 0.05$) (Figure 3c and d). The collagen I to collagen III ratio was also significantly elevated in GzmK$^{-/-}$ wounds compared with WT ($P < 0.05$) (Figure 3c and e). The tensile strength of wounds showed improvement at both days 21 ($P = 0.046$) and 41 after injury ($P = 0.026$) compared with WT controls (Figure 3f).

GzmK impairs healing of wounded keratinocytes

Because classically activated macrophages secrete GzmK (Figure 1e), we investigated the downstream effects of GzmK in vitro in human HaCaTs (keratinocytes) and primary human skin fibroblasts, the predominating cell types in skin. Addition of recombinant human GzmK (rhGzmK) to cells ($\leq$100 nmol/L) showed no detectable cytotoxicity up to 48 hours in culture (see Supplementary Figure S2 online), as previously reported in endothelial cells (Sharma et al., 2016) and lung fibroblasts (Cooper et al., 2011). Using an electric cell-substrate impedance sensing wound healing assay, rhGzmK exhibited a dose-dependent and reproducible impairment of wound closure in HaCaTs, which was approximately 50% slower compared with untreated controls (Figure 4a). Improved HaCaT migration in the absence of GzmK may help explain the improved re-epithelialization observed in GzmK$^{-/-}$ compared with WT mice burns. In contrast to HaCaTs, skin fibroblasts showed no change in wound closure in response to rhGzmK.

GzmK induces PAR-1–mediated proinflammatory cytokine release from keratinocytes, skin fibroblasts, and classically activated macrophages

rhGzmK induces proinflammatory cytokine expression in both endothelial cells and lung fibroblasts, functioning through a PAR-1–mediated pathway (Cooper et al., 2011; Sharma et al., 2016). Studies were therefore performed to determine whether GzmK exposure in HaCaTs and skin fibroblasts induced proinflammatory cytokine expression in a similar fashion, thus providing mechanistic details regarding GzmK's role in burn wound repair. rhGzmK significantly increased IL-6 secretion from both HaCaTs ($P < 0.005$ at $\geq$ 10 nmol/L) (Figure 4b) and skin fibroblasts ($P < 0.005$ at $\geq$ 10 nmol/L) (Figure 4d) in a dose-dependent manner, with each secreting similar amounts. When cells were pre-incubated for 30 minutes with ATAP-2 (5 μg/ml), a PAR-1 neutralizing antibody, before rhGzmK (50 nmol/L) treatment, significant reductions in IL-6 secretion from HaCaTs ($P < 0.005$) (Figure 4c) and a complete amelioration of GzmK-mediated skin fibroblast IL-6 secretion ($P < 0.005$) (Figure 4e) were observed compared with untreated controls.

GzmK induces lipopolysaccharide-activated primary mouse macrophages to process and secrete the proinflammatory cytokine IL-1β (Joeckel et al., 2011). In this study, THP-1–derived M0, M1, and M2a macrophages were exposed to rhGzmK in the absence of perforin, and IL-1β secretion was determined. Cells treated with up to 100 nmol/L rhGzmK showed no evidence of cytotoxicity (see Supplementary Figure S2). Untreated M1 secreted IL-1β, whereas incubation with rhGzmK (50 nmol/L) significantly increased IL-1β release ($P < 0.005$) (Figure 4f). M0 or M2a did not release IL-1β with or without exposure to rhGzmK. Pre-incubation of M1 macrophages with the PAR-1 antagonist ATAP-2 (5 μg/ml) before the addition of rhGzmK (50 nmol/L) ameliorated the GzmK-mediated release of IL-1β (Figure 4g), suggesting that GzmK-mediated IL-1β secretion

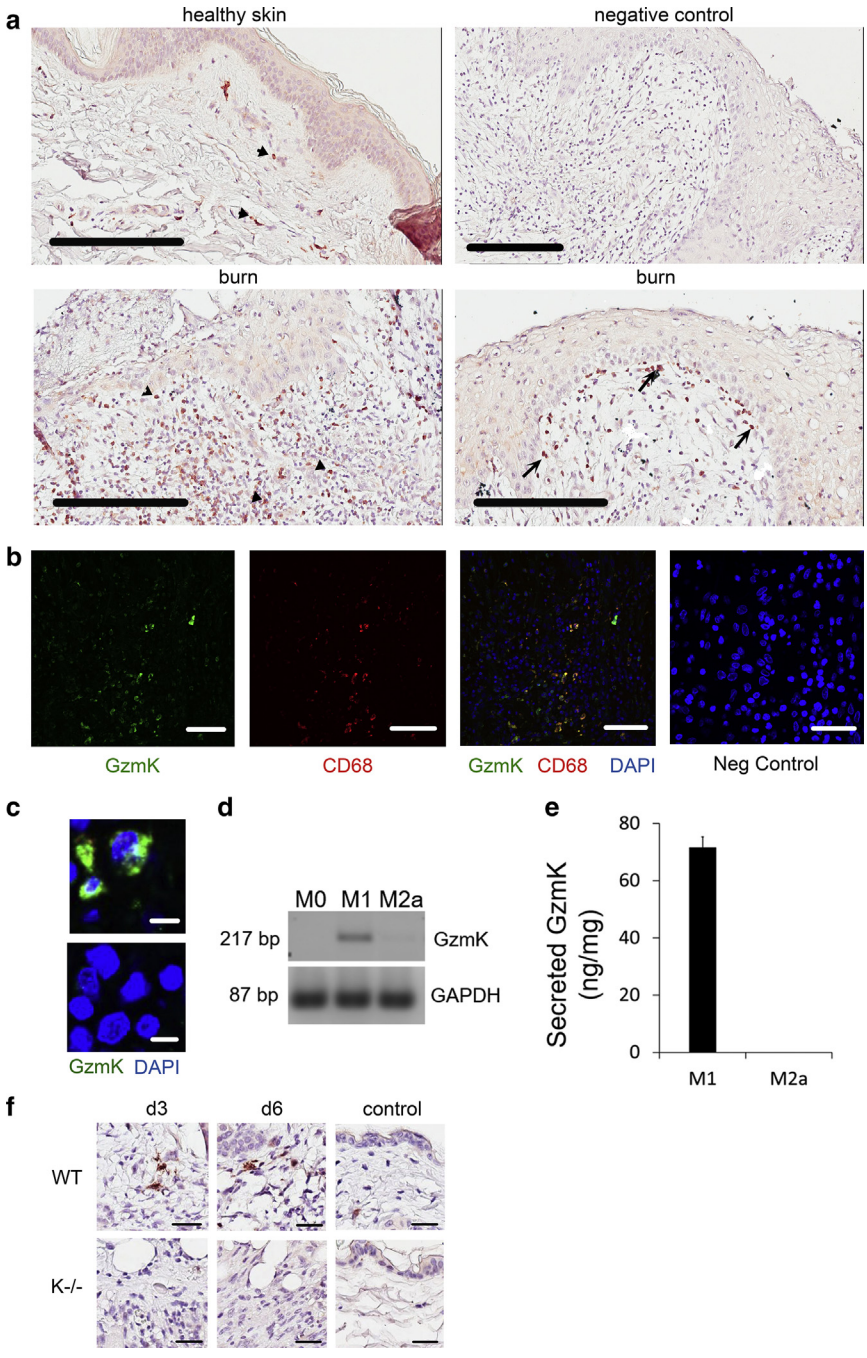

Figure 1. GzmK was elevated in human burns. (**a, b**) Images from patient 2 (day 21 after injury). (**a**) GzmK immunohistochemistry. GzmK$^+$ cells were associated with inflammatory cell infiltrate (arrowheads) and dermal-epidermal junction (arrows). Scale bars = 200 μm. (**b**) GzmK co-localized with CD68 in human burn inflammatory cell infiltrate. Yellow indicates GzmK/CD68 co-localization. Scale bars = 50 μm. Negative controls (**a**, **b**, and **f**) are secondary antibodies only. (**c**) GzmK immunofluorescence in THP-1 cells polarized to M0, then classically (M1) or alternatively (M2a) activated. Scale bars = 10 μm. (**d**) Reverse transcriptase-PCR of macrophage mRNA. (**e**) ELISA GzmK detection in culture supernatants 24 hours after incubation in serum-free medium (ng GzmK/mg total cell protein). Mean ± standard deviation (n = 3 per group). (**f**) GzmK immunohistochemistry in mice burns. Scale bars = 20 μm. bp, base pair; d, day; GzmK, granzyme K; Neg, negative; WT, wild type.

from macrophages is PAR-1 dependent. No effect on IL-1β secretion in response to pre-incubation of cells with ATAP-2 alone was observed.

GzmK augments proinflammatory cytokine expression in mice burn wounds

GzmK$^{-/-}$ mice wounds at day 3 after injury showed significantly reduced IL-6 protein compared with WT controls ($P < 0.05$) (Figure 5a). At day 6 after injury, this pattern was reversed, trending to increased IL-6 protein ($P = 0.062$). IL-1β protein concentration showed no difference at day 3 but was significantly reduced in GzmK$^{-/-}$ mice burns at day 6 after injury ($P = 0.014$).

Augmented chemokine and adhesion molecule expression in GzmK$^{-/-}$ mice burn wounds

Endothelial cells cultured with rhGzmK show increased MCP-1, ICAM-1, and VCAM-1 expression (Sharma et al., 2016); thus, gene expression of each was quantified in mouse burn wounds. MCP-1 ($P = 0.035$), ICAM-1 ($P = 0.0049$), and VCAM-1 ($P = 0.0017$) expressions in GzmK$^{-/-}$ mice at day 3 after injury were significantly reduced compared with those in WT mice (Figure 5b). At day 6, and opposite to the pattern observed at day 3, MCP-1 ($P = 0.025$), ICAM-1 (nonsignificant, $P = 0.2$), and VCAM-1 ($P = 0.023$) expressions were increased in GzmK$^{-/-}$ mice.

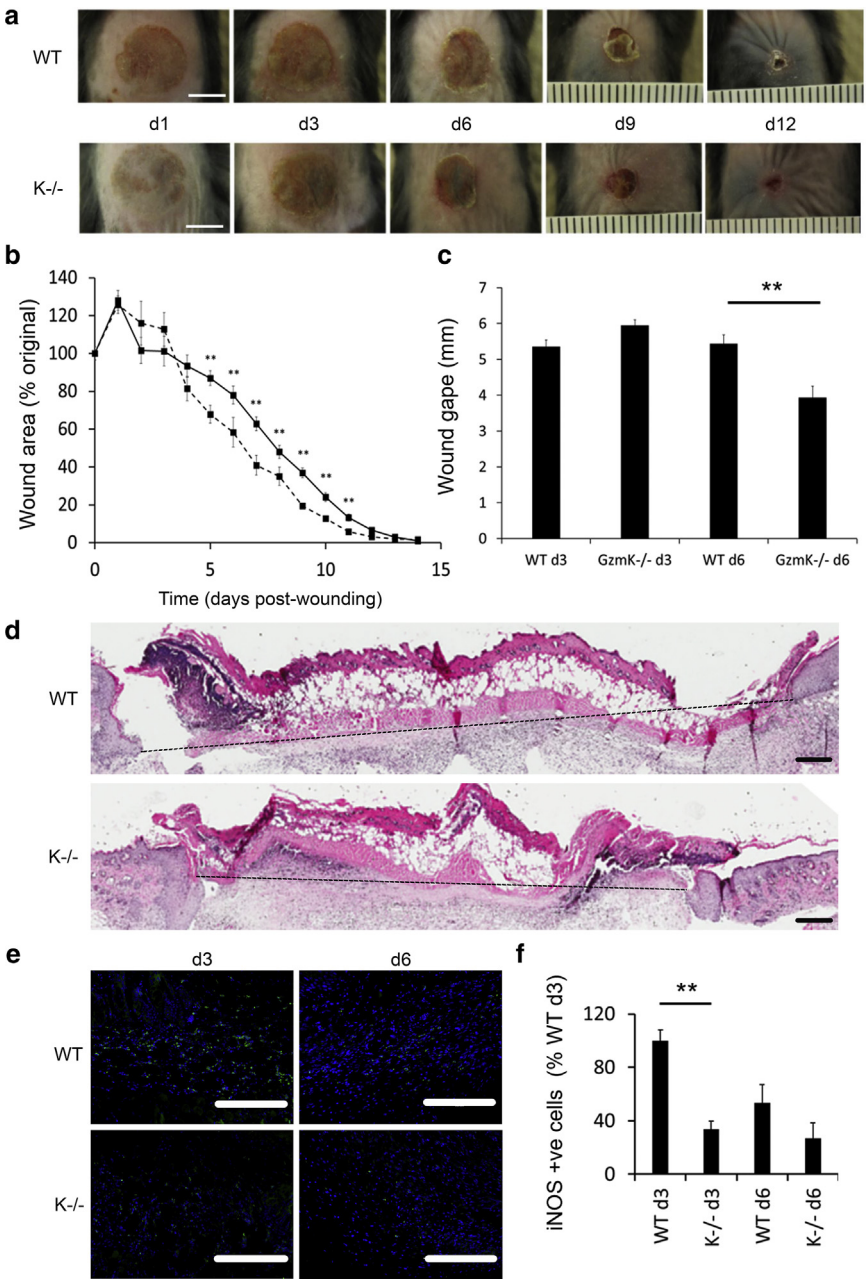

Figure 2. GzmK$^{-/-}$ mice show improved wound healing. (**a**) Photographic comparison of thermal injuries in GzmK$^{-/-}$ and WT mice. Scale bars = 5 mm. (**b**) Quantitative analysis of macroscopic wound area. GzmK$^{-/-}$ (dashed line) and WT (solid line) mice. Data are presented as mean ± standard error of the mean, n ≥ 6 mice per group. (**c**) Quantitative analysis of wound gape as measured from hematoxylin and eosin-stained slides. Data are presented as mean ± standard error of the mean, n = 5 per group. (**d**) Representative hematoxylin and eosin images of wounds at day 6 after injury. Scale bars = 200 μm. (**e**) iNOS (M1 macrophage) staining. Scale bars = 200 μm. (**f**) M1 macrophage quantification. Data are presented as mean ± standard error of the mean, n = 5 per group. *$P < 0.05$, **$P < 0.005$, compared with WT controls and calculated by Student *t* test. d, day; GzmK, granzyme K; iNOS, inducible nitric oxide synthase; WT, wild type.

GzmK increases M1 macrophage recruitment to mice burn wounds

No difference in the amount of inflammatory cell infiltrate was detected between GzmK$^{-/-}$ and WT mice at both days 3 and 6 after injury (Figure 5c). However, macrophage/monocyte and NK cell numbers were significantly reduced in GzmK$^{-/-}$ mice at day 3 after injury compared with WT burns ($P < 0.05$), whereas no change was evident in T cells. In contrast, at day 6, GzmK$^{-/-}$ mice showed an increase in T cells ($P < 0.05$), NK cells ($P < 0.05$), and macrophages/monocytes (not significant, $P = 0.12$) compared with WT mice. Because M1 are the predominant macrophage subtype expressing GzmK in human burns, inducible nitric oxide synthase-positive cells were therefore quantified in mice burns. The number of M1 macrophages was reduced in GzmK$^{-/-}$ compared with WT burns at days 3 ($P < 0.005$) and 6 (nonsignificant) after injury (Figure 2e and f).

DISCUSSION

Nonfatal burns are a major cause of morbidity, leading to prolonged hospitalization, disfigurement, and disability. In the United States alone, more than 400,000 burn injuries occur each year, with approximately 20,000 of those requiring hospitalization (Peck, 2011). Limited therapeutic options are available; consequently, new targeted strategies are required. Reducing the magnitude of inflammation immediately after injury has been identified as one such target (Farina et al., 2013).

This study shows that GzmK is abundant in burn wounds and plays a pathogenic role in inflammation,

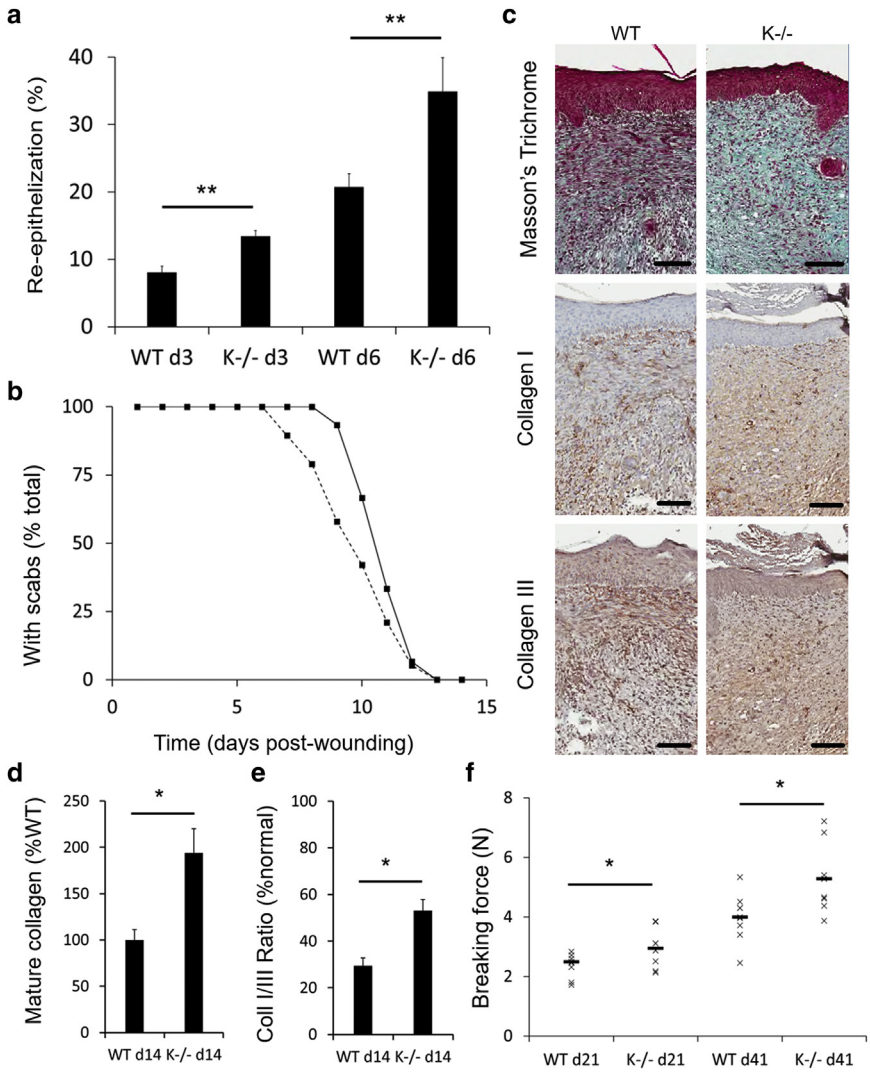

Figure 3. GzmK$^{-/-}$ mice show improved re-epithelialization and tissue repair. (**a**) Re-epithelialization of burns after injury. (**b**) Scabs falling off provides an indirect re-epithelialization measure. GzmK$^{-/-}$ (dashed line, n = 18) and WT (solid line, n = 15). (**c**) Representative Masson's trichrome, collagen I, and collagen III staining in mouse burn granulation tissue (day 14 after injury, n = 6). Scale bar = 100 μm. (**d**) Masson's trichrome quantification and (**e**) collagen I/III ratio. (**f**) Minimum wound breaking force at days 21 and 41 after injury, n ≥ 6 mice per group. Data in **a**, **d**, and **e** are presented as mean ± standard error of the mean, n ≥ 5 mice per group. (**f**) Mean plus each individual data point. n ≥ 5 mice per group. *$P < 0.05$, **$P < 0.005$ compared with WT and calculated by Student *t* test. d, day; GzmK, granzyme K; WT, wild type.

epithelialization, and remodeling. Previously, GzmK expression was reported in cytotoxic T lymphocytes, NK, and CD4$^+$ T cells (Joeckel et al., 2011, 2012, 2017; Wilson et al., 2017). Our data suggest that in burn wounds, GzmK is predominantly localized to the CD68$^+$ monocyte/macrophage cell populations within the dermis. Differentially polarized, proinflammatory/pro-reparative macrophages have been described, with both anti-inflammatory and proinflammatory cytokine expression reported to be induced simultaneously at early time points during tissue repair (Murray, 2017). In our studies, classically activated M1 macrophages expressed and secreted GzmK, whereas M2a macrophages exhibited negligible GzmK expression. Thus, GzmK may contribute to the proinflammatory response after burn injury.

Thermal injury in GzmK$^{-/-}$ mice exhibited improved overall wound healing, enhanced re-epithelialization, improved dermal maturation, and stronger tensile strength compared with WT mice wounds. Re-epithelialization was particularly striking in GzmK$^{-/-}$ compared with WT mice burns. The epithelial tongues in GzmK$^{-/-}$ mice exceeded double the length of those in WT mice as early as day 3 after injury. In vitro, GzmK impaired keratinocyte wound closure, suggesting a direct effect on cellular migration. Rapid re-epithelialization and wound closure greatly benefits overall wound healing, in part by re-establishing a barrier against infection, a major contributor to wounds transitioning into chronicity. The downside of increasing cell proliferation and migration during wound repair is the potential to induce fibrosis. The GzmK-mediated reduction in cell migration observed in our study, however, was limited to cultured keratinocytes, whereas fibroblasts, the major cell type involved in fibrosis, showed no alteration in response to GzmK exposure. Currently, the mechanism of GzmK-mediated inhibition of keratinocyte proliferation remains elusive and is an active area of investigation.

Proinflammatory IL-6, essential for timely wound healing, is involved in generating acute phase responses, inflammation, and lymphocyte differentiation (McFarland-Mancini et al., 2010). GzmK-mediated IL-6 secretion occurs in endothelial cells (Sharma et al., 2016), and our data showed GzmK-mediated IL-6 secretion from cultured HaCaTs and skin fibroblasts, releasing similar quantities from each, and both operating through PAR-1. Indeed, in GzmK$^{-/-}$ mouse burns at day 3 after injury, IL-6 expression was reduced compared with equivalent

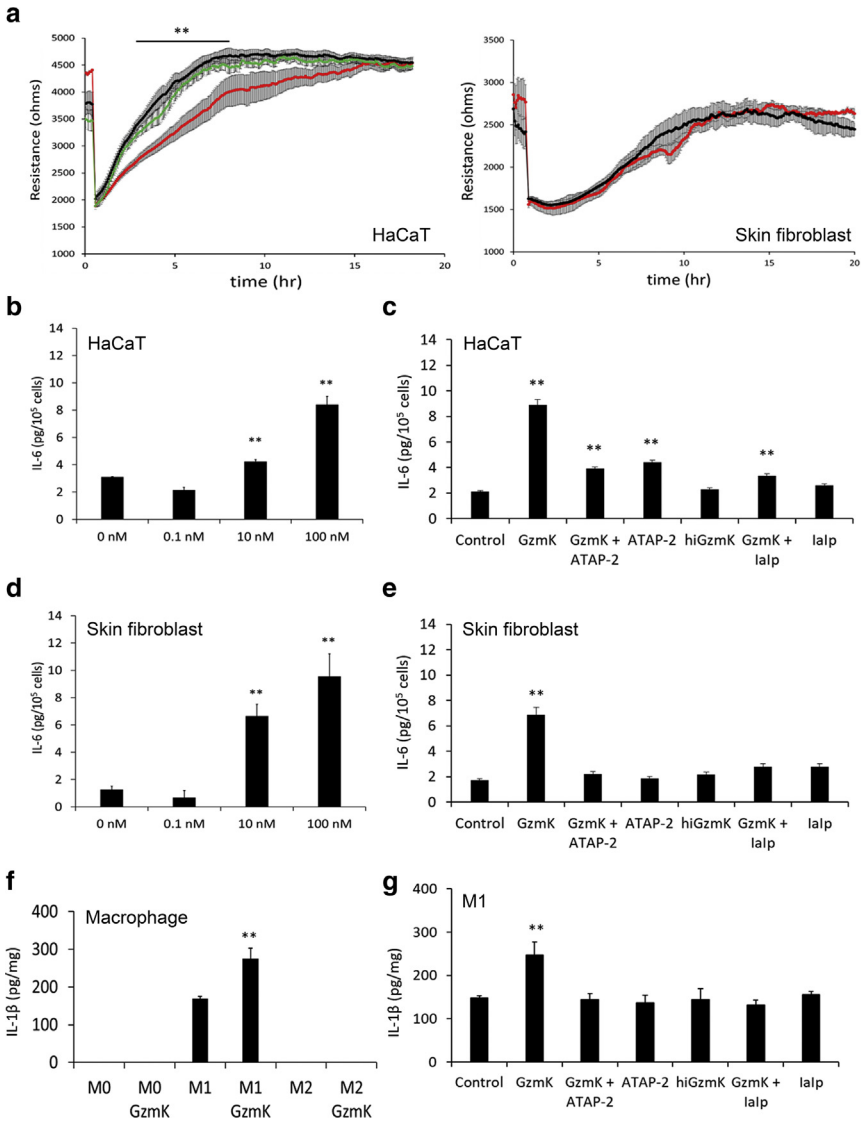

Figure 4. GzmK impairs keratinocyte wound healing in vitro and induces proinflammatory cytokine expression. (**a**) ECIS wound assay. Cells incubated with 10 nmol/L (green, 300 ng/ml), 25 nmol/L (red, 600 ng/ml) rhGzmK or untreated (black), n = 3, performed three times. (**b**–**e**) IL-6 ELISA of cell supernatants. (**f, g**) IL-1β ELISA of macrophage supernatants. Cells in **c**, **e**, **f**, and **g** were incubated with 50 nmol/L rhGzmK. PAR-1 inhibitor ATAP-2 at 5 μg/ml. GzmK inhibitor Iαlp at 4 μmol/L. Presented as mean ± standard deviation (n = 3), performed twice. IL-6 data presented as pg per 10^5 cells, IL-1β as picograms per milligram cell protein. $^*P < 0.05$, $^{**}P < 0.005$ compared with untreated by Student *t* test, except for two-way analysis of variance in **a**. ECIS, electric cell-substrate impedance sensing; GzmK, granzyme K; hiGzmK, heat-inactivated GzmK; hr, hour; M, mol/L.

WT samples. This trend appeared to be reversed by day 6, suggesting that the absence of GzmK may contribute to a delayed proinflammatory profile in response to thermal injury.

Joeckel et al. (2011) previously reported GzmK-mediated IL-1β secretion from lipopolysaccharide activated macrophages, with this predicted to be inflammasome dependent (Joeckel et al., 2011). Our data confirmed GzmK-mediated IL-1β secretion from classically activated macrophages, showing PAR-1 dependent release. Because IL-1β has an important role in wound healing, providing a positive feedback loop capable of sustaining a persistent proinflammatory wound phenotype (Mirza et al., 2013), we investigated the effect of GzmK knockout on IL-1β expression after thermal injury. Although there was no difference at day 3 after injury, IL-1β expression was significantly reduced in GzmK$^{-/-}$ burn wounds at day 6. GzmK therefore appears to play a role in either delaying or possibly reducing the proinflammatory IL-1β profile, which may in turn decrease macrophage recruitment after burn injury.

GzmK induces MCP-1, ICAM-1, and VCAM-1 expression in endothelial cells (Sharma et al., 2016), with these factors together facilitating immune cell adhesion and transendothelial migration (Ley et al., 2007). GzmK increased adhesion of THP-1 monocytes to cultured endothelial cells (Sharma et al., 2016), suggesting that GzmK may directly affect immune cell recruitment. In this study, MCP-1, ICAM-1, and VCAM-1 gene expression were significantly reduced at day 3 after injury in GzmK$^{-/-}$ compared with WT mouse wounds, corresponding to a reduction in both macrophages and NK cells in the wound environment. Previously, GzmK$^{-/-}$ mice infected with Chikungunya virus, showing a significant reduction in foot swelling, had no overall change in inflammatory cell infiltrate or macrophage numbers, but NK and T cells were both reduced (Wilson et al., 2017). Our day 3 postinjury data also showed no change in overall inflammatory cell or T-cell recruitment and a reduction in NK cells. The reason for different macrophage recruitment between these studies remains unknown but can be explained by differences in the pathologies. At day 6 after injury, the pattern of MCP-1, ICAM-1, and VCAM-1 expression was reversed to that seen at day 3, showing an increase in the GzmK$^{-/-}$ mice, and suggesting that the proinflammatory

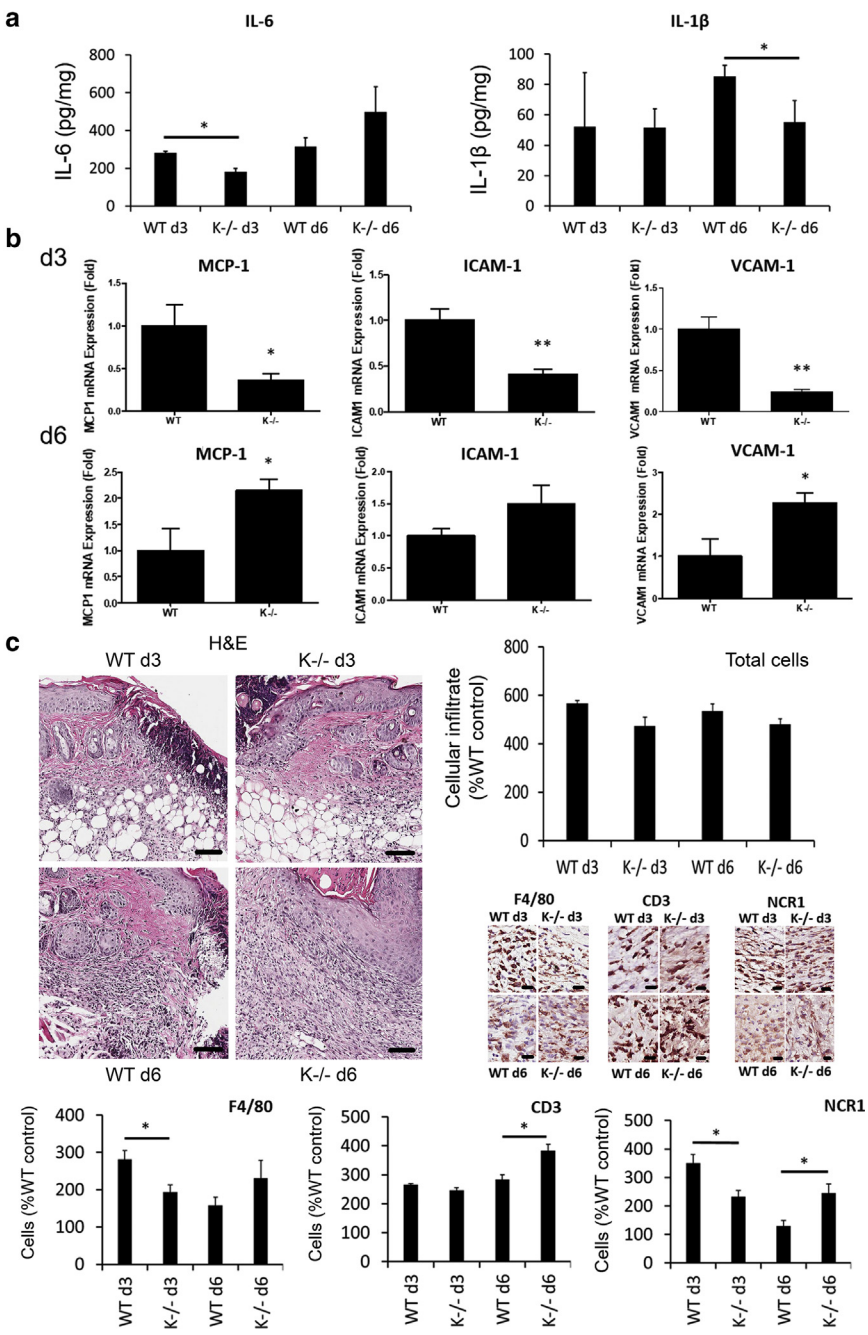

Figure 5. Altered inflammatory cell infiltration and cytokine expression in murine burn wounds. (**a**) ELISA detection of proinflammatory cytokines in mice burn tissue. Data are presented as picograms per milliliter cell protein, n ≥ 3 per group. (**b**) Gene expression in mice burn tissue at days 3 and 6 after injury. Data are presented as fold increase over WT samples, n ≥ 3 per group. (**c**) Inflammatory cell infiltrate, F4/80- (macrophages), CD3- (T cells), and NCR1- (NK cells) positive cells in mouse burn tissue at days 3 and 6 after injury. Scale bars = 100 μm (H&E) and 15 μm (immunohistochemistry). Data are presented as percentage of cells relative to WT unwounded skin controls, showing mean ± standard deviation. n = 6. *$P < 0.05$, **$P <$ 0.005 compared with WT; statistics by two-way analysis of variance. d, day; H&E, hematoxylin and eosin; NK, natural killer; WT, wild type.

response is not reduced but rather delayed after burn injury, and agreeing with the proinflammatory IL-6 expression data.

In conclusion, GzmK delays burn wound healing by impairing re-epithelialization and promoting proinflammatory cytokine expression and subsequent immune cell recruitment to the site of injury (Figure 6). This study suggests that GzmK could be targeted to attenuate inflammation and promote epithelialization in the context of burn injury.

MATERIALS AND METHODS

Human samples

Normal human skin and acute burns were obtained from Vancouver General Hospital Burns Clinic with approval from the University of British Columbia Human Research Ethics Committee (H12-00540), and after obtaining written, informed patient consent. Samples were fixed in 10% (volume/volume) neutral buffered formalin for histology and/or immunofluorescence microscopy.

Cell culture

THP-1 monocytes were cultured and polarized into M0, M1, and M2a macrophages, as described previously (Genin et al., 2015). Primary human skin fibroblasts were from skin biopsy samples donated by apparently healthy volunteers. Fibroblasts and HaCaT cells were maintained in DMEM containing 10% (volume/volume) fetal bovine serum and 1% (volume/volume) penicillin/streptomycin from Sigma-Aldrich (St. Louis, MO). Cells were cultured in serum-free (HaCaTs) or low serum (2% heat inactivated fetal bovine

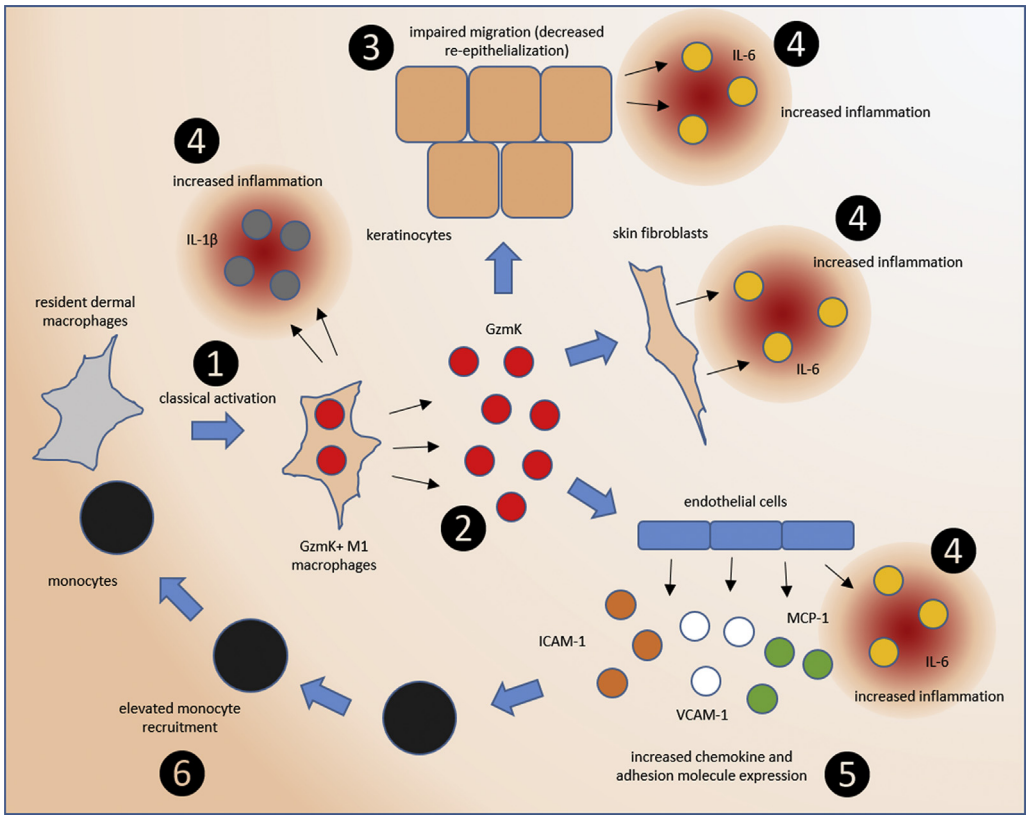

Figure 6. Mechanism of GzmK in impaired thermal injury repair. After thermal injury in skin, monocytes and resident dermal macrophages are recruited to the site of injury and classically activated (1). GzmK expression is up-regulated in M1, with some secreted into the wound area (2). GzmK inhibits re-epithelialization (3) and induces proinflammatory cytokine release from M1 macrophages, keratinocytes, skin fibroblasts, and endothelial cells (4). Endothelial cells also secrete chemokines and adhesion molecules in response to GzmK exposure (5), leading to an up-regulation of monocyte recruitment to the wound (6). Together, GzmK induces an enhanced burn induced proinflammatory response, contributing to a delay in wound healing. GzmK, granzyme K.

serum, fibroblasts and macrophages) medium conditions before and during each experiment.

Quantitative PCR

RNA was isolated using Trizol reagent as per the manufacturer's directions (Invitrogen, Burlington, Ontario, Canada). DNase I treatment removed contaminating genomic DNA. cDNA synthesis required random hexamers and M-MuLV reverse transcriptase. cDNA reactions were incubated for 5 minutes at room temperature, 42 °C for 60 minutes, and 65 °C for 20 minutes to inactivate the enzyme. Quantitative PCR used PowerUp SYBR master mix on a ViiA in duplicate using primers against ICAM1 (forward: 5′-CTCG AGAGTGGACCCAACTGGAAG-3′ reverse: 5′-CAGGCTGGCAGAG GTCTCAG-3′), VCAM1 (forward: 5′-GAACACTCTTACCTGTGCAC AGC-3′ reverse: 5′-CTTGACCGTGACCGGCTTCC-3′), MCP1 (forward: 5′-AACGCCCCACTCACCTGCTG-3′ reverse: 5′-CCTTCTTGG GGTCAGCACAG-3′), and GAPDH (forward: 5′-TGCACCACCAA CTGCTTAGC-3′ reverse: 5′-GGCATGGACTGTGGTCATGAG-3′). Cycling conditions were 50 °C 2 minutes ×1, 95 °C 5 minutes ×1, 95 °C 15 seconds, 60 °C 30 seconds ×40. mRNA levels were normalized to GAPDH and compared with WT mice.

Reverse transcriptase-PCR

Total RNA and cDNA synthesis from macrophages was accomplished as described. Human granzyme K was amplified using a Bio-Rad (Hercules, CA) T100; (forward: 5′-CCTAATAGTTGGGGCTTA-TATGAC-3′ reverse: 5′-GCCTAAAACCACAGTGGGAG-3′). Thermocycling was as follows: 95 °C 5 minutes ×1, 95 °C 15 seconds, 61 °C 45 seconds ×40, 61 °C 2 minutes. Amplification of GAPDH was used as control. PCR products were separated on a 2% agarose gel and visualized using a LI-COR (Lincoln, NE) Odyssey Fc system under the 600-nm channel.

Immunohistochemistry and immunofluorescence microscopy

Immunohistochemistry and immunofluorescence microscopy were performed as previously described (Shen et al., 2012), using antibodies as listed in Supplementary Table S2 online.

Morphometric analysis

Re-epithelialization was measured as (distance of new epithelium from leading edges to wound margins)/(distance of wound bed) × 100. Presence of total macrophages, M1 macrophages, T cells, and NK cells were determined by staining intensity in two representative rectangles of 200 × 160 μm^2 in the granulation tissue of wound sections (minimum of five wounds on six mice per time point for each group). Data presented as the number of positively stained cells in wounded tissue as a percentage of positively stained cells in WT unwounded skin. There was no difference in cell number between unwounded WT and GzmK$^{-/-}$ skin. Inflammatory infiltrates were characterized by high density blue nuclear staining; thus, total infiltrate was measured by ratio of blue (nuclear) to red (cytoplasmic) staining (Poo et al., 2014; Wilson et al., 2017).

Electric cell-substrate impedance sensing

The electrical properties of confluent and wounded fibroblasts and keratinocytes were examined using electric cell-substrate impedance sensing (Applied Biophysics, Troy, NY), applying the wound assay function as previously described (Turner et al., 2017b). Briefly, cells were seeded into 8W1E PET electric cell-substrate impedance sensing Cultureware arrays (Applied Biophysics) and maintained until confluence. Wells were rinsed twice with phosphate buffered saline (pH 7.2), then incubated for 1 hour in fetal bovine serum-free DMEM before rhGzmK-treatment (10 nmol/L low dose, 25 nmol/L high dose) in fetal bovine serum-free DMEM. At 1 hour, array sensors were wounded at 2,500 μA, 48,000 Hz for 20 seconds. Wound

recovery was determined in real time by impedance (36,000 Hz), with recovery defined as the time taken for the signal to plateau.

ELISA

Kit ELISAs were used to evaluate human IL-6 (Human DuoSet ELISA DY206; R&D Systems, Minneapolis, MN), mouse IL-6 (Rab0309; Sigma-Aldrich, St. Louis, MO), human IL-1β (ab100562; Abcam, Cambridge, MA), mouse IL-1β (ab100705, Abcam), and GzmK (LSBio, Seattle, WA) in serum-free supernatant from fibroblasts, keratinocytes, and macrophage or tissue extracts.

Animal studies

All procedures were performed in accordance with the guidelines approved by the Animal Experimentation Committee, University of British Columbia (A17-0024). GzmK$^{-/-}$ mice (C57Bl/6 background) were generated as described (Joeckel et al., 2017). GzmK$^{-/-}$ mice showed no phenotypic differences to WT mice, including in anatomy, health, fecundity, litter size, and hematopoietic development (Joeckel et al., 2017). C57Bl/6 WT mice were obtained from Jackson Laboratories (Bar Harbor, ME) and acclimatized for 2 weeks before experimental procedures began. Six female mice were (7−10 weeks of age) included per treatment group.

Murine thermal injury techniques

Mice were anaesthetized with inhaled isoflurane, and the dorsum was shaved and cleaned with 10% (weight/volume) povidine iodine solution. Thermal injuries were performed by placement of a 6-mm−diameter metal rod, heated for 10 minutes in boiling water, on the dorsum for 6 seconds. Digital photographs were captured daily using a ruler aligned next to the wound, allowing direct wound measurements to be made. Wounds were harvested at days 3, 6, and 14 and bisected. One half was fixed in 10% (volume/volume) buffered formalin and processed so that the midpoint of the wound was sectioned and compared between groups. The other half was snap frozen in liquid nitrogen for protein extraction. Additional wounds were harvested at days 21 and 41 for skin tensiometry.

Skin tensiometry

The tensile breaking force of burn-wounded skin was evaluated using the Mecmesin Motorised Force Tester (Mecmesin Corporation, Slinfold, UK), similar to what has been reported previously (Kopecki et al., 2013). Briefly, excised skin (1 × 4 cm, wounded area in the center) was attached to a 200-N Spring Action Vice Clamp (Mecmesin Corporation, Slinfold, UK) and pulled apart at 3 cm/minute using the MultiTest 2.5-d Test System Stand (Mecmesin Corporation, Slinfold, UK). Tensile strength was assessed with an Advanced Force Gauge 100N (Mecmesin Corporation, Slinfold, UK) and recorded in real time using Emperor Lite software (Mecmesin). Tensile strength was assessed as the minimum force required to cause skin breakage.

Statistical analysis

Statistical differences were determined using Student *t* test or two-way analysis of variance. For data not following a normal distribution, the Mann-Whitney *U* test was performed. *P*-values less than 0.05 were considered significant.

ORCIDs

Christopher T Turner: http://orcid.org/0000-0001-7409-4386
Matthew R Zeglinski: http://orcid.org/0000-0002-3858-5791

CONFLICT OF INTEREST

DJG is co-founder of viDA Therapeutics, Inc. However, no viDA reagents were used in this study.

ACKNOWLEDGMENTS

The authors acknowledge funding support from Mitacs (to CTT), fellowships from the Canadian Institutes for Health Research (CIHR) (to CTT and MRZ), grants-in-aid from CIHR (to DJG), the Michael Smith Foundation for Health Research (to DJG and MRZ), and the Rick Hansen Institute (to DJG).

SUPPLEMENTARY MATERIAL

Supplementary material is linked to the online version of the paper at www.jidonline.org, and at https://doi.org/10.1016/j.jid.2018.09.031.

REFERENCES

Bade B, Lohrmann J, ten Brinke A, Wolbink AM, Wolbink GJ, ten Berge IJ, et al. Detection of soluble human granzyme K in vitro and in vivo. Eur J Immunol 2005;35:2940−8.

Bratke K, Klug A, Julius P, Kuepper M, Lommatzsch M, Sparmann G, et al. Granzyme K: a novel mediator in acute airway inflammation. Thorax 2008;63:1006−11.

Cooper DM, Pechkovsky DV, Hackett TL, Knight DA, Granville DJ. Granzyme K activates protease-activated receptor-1. PLoS One 2011;6(6):e21484.

Farina JA Jr, Rosique MJ, Rosique RG. Curbing inflammation in burn patients. Int J Inflam 2013;2013:715645.

Genin M, Clement F, Fattaccioli A, Raes M, Michiels C. M1 and M2 macrophages derived from THP-1 cells differentially modulate the response of cancer cells to etoposide. BMC Cancer 2015;15:577.

Joeckel LT, Allison CC, Pellegrini M, Bird CH, Bird PI. Granzyme K-deficient mice show no evidence of impaired antiviral immunity. Immunol Cell Biol 2017;95:676−83.

Joeckel LT, Wallich R, Martin P, Sanchez-Martinez D, Weber FC, Martin SF, et al. Mouse granzyme K has pro-inflammatory potential. Cell Death Differ 2011;18:1112−9.

Joeckel LT, Wallich R, Metkar SS, Froelich CJ, Simon MM, Borner C. Interleukin-1R signaling is essential for induction of proapoptotic CD8 T cells, viral clearance, and pathology during lymphocytic choriomeningitis virus infection in mice. J Virol 2012;86:8713−9.

Kopecki Z, Ruzehaji N, Turner C, Iwata H, Ludwig RJ, Zillikens D, et al. Topically applied flightless I neutralizing antibodies improve healing of blistered skin in a murine model of epidermolysis bullosa acquisita. J Invest Dermatol 2013;133:1008−16.

Ley K, Laudanna C, Cybulsky MI, Nourshargh S. Getting to the site of inflammation: the leukocyte adhesion cascade updated. Nat Rev Immunol 2007;7:678−89.

Lobe CG, Finlay BB, Paranchych W, Paetkau VH, Bleackley RC. Novel serine proteases encoded by two cytotoxic T lymphocyte-specific genes. Science 1986;232(4752):858−61.

Masson D, Tschopp J. A family of serine esterases in lytic granules of cytolytic T lymphocytes. Cell 1987;49:679−85.

McFarland-Mancini MM, Funk HM, Paluch AM, Zhou M, Giridhar PV, Mercer CA, et al. Differences in wound healing in mice with deficiency of IL-6 versus IL-6 receptor. J Immunol 2010;184:7219−28.

Mirza RE, Fang MM, Ennis WJ, Koh TJ. Blocking interleukin-1β induces a healing-associated wound macrophage phenotype and improves healing in type 2 diabetes. Diabetes 2013;62:2579−87.

Murray PJ. Macrophage polarization. Annu Rev Physiol 2017;79:541−66.

Peck MD. Epidemiology of burns throughout the world. Part I: distribution and risk factors. Burns 2011;37:1087−100.

Poo YS, Rudd PA, Gardner J, Wilson JA, Larcher T, Colle MA, et al. Multiple immune factors are involved in controlling acute and chronic chikungunya virus infection. PLoS Negl Trop Dis 2014;8(12):e3354.

Rucevic M, Fast LD, Jay GD, Trespalcios FM, Sucov A, Siryaporn E, et al. Altered levels and molecular forms of granzyme K in plasma from septic patients. Shock 2007;27:488−93.

Sharma M, Merkulova Y, Raithatha S, Parkinson LG, Shen Y, Cooper D, et al. Extracellular granzyme K mediates endothelial activation through the cleavage of protease-activated receptor-1. FEBS J 2016;283:1734−47.

Shen Y, Guo Y, Mikus P, Sulniute R, Wilczynska M, Ny T, et al. Plasminogen is a key proinflammatory regulator that accelerates the healing of acute and diabetic wounds. Blood 2012;119:5879−87.

Tschopp J, Masson D, Schafer S. Inhibition of the lytic activity of perforin by lipoproteins. J Immunol 1986;137:1950–3.

Turner CT, Lim D, Granville DJ. Granzyme B in skin inflammation and disease [e-pub ahead of print]. Matrix Biol 2017a. https://doi.org/10.1016/j.matbio.2017.12.005 (accessed 11 October 2018).

Turner CT, McInnes SJ, Melville E, Cowin AJ, Voelcker NH. Delivery of flightless I neutralizing antibody from porous silicon nanoparticles improves wound healing in diabetic mice. Adv Healthc Mater 2017b;6(2):1600707.

Voskoboinik I, Whisstock JC, Trapani JA. Perforin and granzymes: function, dysfunction and human pathology. Nat Rev Immunol 2015;15:388–400.

Wensink AC, Wiewel MA, Jongeneel LH, Boes M, Van der Poll T, Hack CE, et al. Granzyme M and K release in human experimental endotoxemia. Immunobiology 2016;221:773–7.

Wilson JA, Prow NA, Schroder WA, Ellis JJ, Cumming HE, Gearing LJ, et al. RNA-Seq analysis of chikungunya virus infection and identification of granzyme A as a major promoter of arthritic inflammation. PLoS Pathog 2017;13(2):e1006155.